

# Recent results on light hadron spectroscopy from BES II \*

SHEN Xiao-Yan(沈肖雁)<sup>1)</sup> (for the BES Collaboration)

(Institute of High Energy Physics, CAS, Beijing 100049, China)

**Abstract** We reported the observation of  $Y(2175)$  in  $\phi f_0(980)$  mass spectrum in  $J/\psi \rightarrow \eta \phi f_0(980)$  with  $f_0(980) \rightarrow \pi^+ \pi^-$  and the observation of a broad  $1^{--}$  resonance of  $K^+ K^-$  mass in  $J/\psi \rightarrow K^+ K^- \pi^0$ . The results from the partial wave analyses of  $J/\psi \rightarrow \gamma \pi^+ \pi^-$  and  $\gamma \pi^0 \pi^0$ , as well as  $J/\psi \rightarrow p K^- \bar{\Lambda}$  are also presented.

**Key words**  $J/\psi$  decay, invariant mass spectrum, resonance, partial wave analysis

**PACS** 13.25.Gv

## 1 Introduction

QCD predicts the existence of the multi-quark states,  $q\bar{q}$ -gluon hybrids and glueballs. These states have been searched for many years by some experiments. However, none of them is well established after all the efforts. The  $5.8 \times 10^7$   $J/\psi$  data sample, accumulated with BES detector, provides a good laboratory for the search of non- $q\bar{q}$  states and study of light hadron spectroscopy.

## 2 Observation of $Y(2175)$ in $J/\psi \rightarrow \eta \phi f_0(980)$

A new  $1^{--}$  structure, denoted as  $Y(2175)$  and with mass  $m = 2.175 \pm 0.010 \pm 0.015$   $\text{GeV}/c^2$  and width  $\Gamma = 58 \pm 16 \pm 20$   $\text{MeV}/c^2$ , was observed by the BABAR experiment in the  $e^+ e^- \rightarrow \gamma_{\text{ISR}} \phi f_0(980)$  initial-state radiation (ISR) process<sup>[1, 2]</sup>. This observation stimulated some theoretical speculation that this state may be an s-quark version of the  $Y(4260)$  since both of them are produced in  $e^+ e^-$  annihilation and decay to similar final states<sup>[3]</sup>. The  $Y(2175)$  has correspondingly been interpreted as a  $s\bar{s}g$ <sup>[4]</sup>, a  $2^3D_1$   $s\bar{s}$  state<sup>[5]</sup> or a tetraquark  $s\bar{s}s\bar{s}$  state<sup>[6]</sup>. As of now, none of these interpretations have either been established or ruled out by experiment.

With a sample of  $5.8 \times 10^7$   $J/\psi$  events collected with upgraded Beijing Spectrometer (BES II) detector<sup>[7]</sup> at Beijing Electron-Positron Collider

(BEPC), the decays of  $J/\psi \rightarrow \eta \phi f_0(980)$ , with  $\eta \rightarrow \gamma\gamma$ ,  $\phi \rightarrow K^+ K^-$ ,  $f_0(980) \rightarrow \pi^+ \pi^-$  are analyzed. After the final events selection, an  $\eta$  signal is evident in the  $\gamma\gamma$  invariant mass spectrum (Fig. 1(a));  $\eta \rightarrow \gamma\gamma$  candidates are defined as  $\gamma$ -pairs with  $|m_{\gamma\gamma} - 0.547| < 0.037$   $\text{GeV}/c^2$ . A  $\phi$  signal is distinct in the  $K^+ K^-$  invariant mass spectrum (Fig. 1(b)) and for these candidates we require  $|m_{K^+ K^-} - 1.02| < 0.019$   $\text{GeV}/c^2$ .

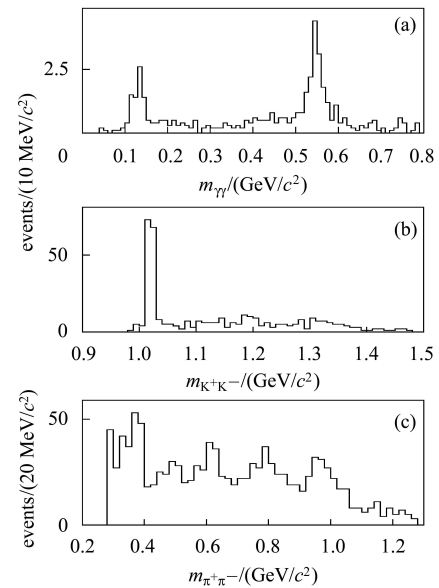


Fig. 1. (a) The  $\gamma\gamma$  invariant mass spectrum. (b) The  $K^+ K^-$  invariant mass spectrum. (c) The  $\pi^+ \pi^-$  invariant mass spectrum.

Received 18 January 2008

\* Supported by National Natural Science Foundation of China (10491300, 10225524, 10225525, 10425523, 10625524, 10521003)

1) E-mail: shenxy@ihep.ac.cn

In the  $\pi^+\pi^-$  invariant mass spectrum, candidate  $f_0(980)$  mesons are defined by  $|m_{\pi^+\pi^-} - 0.980| < 0.060$   $\text{GeV}/c^2$  (Fig. 1(c)). The  $\phi f_0(980)$  invariant mass spectrum for the selected events is shown in Fig. 2(a), where a clear enhancement is seen around  $2.18$   $\text{GeV}/c^2$ .

The Dalitz plot of  $m_{\eta f_0(980)}^2$  versus  $m_{\eta\phi}^2$  for the selected events is shown in Fig. 2(b), where a diagonal band can be seen. This band corresponds to the structure observed around  $2.18$   $\text{GeV}/c^2$  in the  $\phi f_0(980)$  invariant mass spectrum shown in Fig. 1(a).

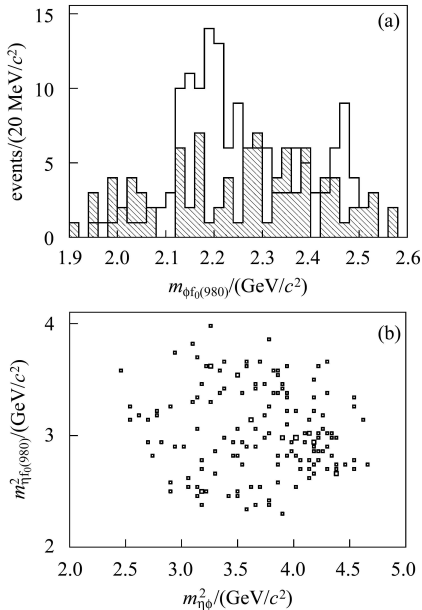


Fig. 2. (a) The  $\phi f_0(980)$  invariant mass spectrum; The open histogram is data and the shaded histogram is sideband-determined background. (b) The Dalitz plot of  $m_{\eta f_0(980)}^2$  versus  $m_{\eta\phi}^2$ .

To clarify the origin of the observed structure, we have made extensive studies of potential background processes using both data and MC. Non- $\eta$  or non- $f_0(980)$  processes are studied with  $\eta$ - $f_0(980)$  mass sideband events. Non- $\phi$  processes are studied with  $\phi$  mass sideband events. The total sideband events estimated from all these sidebands (minus double counting) are shown as the shaded histogram in Fig. 2(a). No structure around  $2.18$   $\text{GeV}/c^2$  is evident.

We fit the  $\phi f_0(980)$  invariant mass spectrum and the total sidebands simultaneously. In the fit, the normalization for the background polynomial is constrained to be the same for both the signal and sideband histograms. We use a constant-width Breit-Wigner (BW) convolved with a Gaussian mass resolution function (with  $\sigma = 12$   $\text{MeV}/c^2$ ) to represent the  $Y(2175)$  signal. The statistical significance of the signal is  $5.5\sigma$ . The mass and width obtained from the fit (shown as smooth curves in Fig. 3) are  $M = 2.186 \pm 0.010(\text{stat}) \pm 0.006(\text{syst})$   $\text{GeV}/c^2$

and  $\Gamma = 0.065 \pm 0.023(\text{stat}) \pm 0.017(\text{syst})$   $\text{GeV}/c^2$ , and the product branching ratio is measured to be  $Br(J/\psi \rightarrow \eta Y(2175)) \cdot Br(Y(2175) \rightarrow \phi f_0(980)) \cdot Br(f_0(980) \rightarrow \pi^+\pi^-) = (3.23 \pm 0.75(\text{stat}) \pm 0.73(\text{syst})) \times 10^{-4}$ , using MC-determined selection efficiency of 1.44%. Here, the second errors are systematic errors. The systematic uncertainties on the mass and width are estimated by varying the function form used to represent the background, the fitting range of the invariant mass spectrum, the bin width of the invariant mass spectrum, allowing the sideband and signal background normalizations to differ and possible fitting biases. The latter are estimated from the differences between the input and output mass and width values from MC studies. In addition to above systematic sources, the systematic error on the branching ratio measurement comes also from the uncertainties of MDC simulation (including systematic uncertainties of the tracking efficiency and the kinematic fits), the photon detection efficiency, the particle identification efficiency, the  $\eta$  decay branching ratio to  $\gamma\gamma$  and the  $\phi$  decay branching ratio to  $K^+K^-$ .

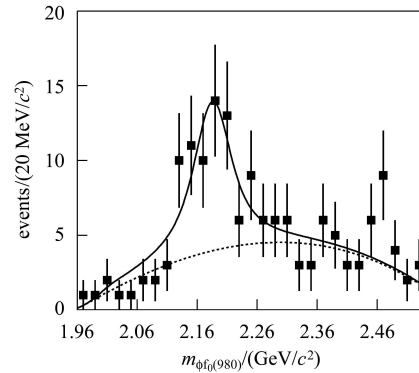


Fig. 3. The solid curve is the fit to the data (points with error bars).

### 3 Observation of a broad $1^{--}$ resonant structure in the $K^+K^-$ mass spectrum in $J/\psi \rightarrow K^+K^-\pi^0$

A broad peak is observed at low  $K^+K^-$  invariant mass in  $J/\psi \rightarrow K^+K^-\pi^0$  decays, detailed analysis is described in Ref. [8].

The Dalitz plot for the selected 10631 events is shown in Fig. 4(b), where a broad  $K^+K^-$  band is evident in addition to the  $K^*(892)$  and  $K^*(1410)$  signals. This band corresponds to the broad peak observed around  $1.5$   $\text{GeV}/c^2$  in the  $K^+K^-$  invariant mass projection shown in Fig. 4(c).

A partial wave analysis shows that the  $J^{PC}$  of this structure is  $1^{--}$ . Its pole position is determined to be  $(1576_{-55}^{+49+98})$   $\text{MeV}/c^2 - i(409_{-12}^{+11+32})$   $\text{MeV}/c^2$ , and the branching ratio is  $B(J/\psi \rightarrow X\pi^0) \cdot B(X \rightarrow K^+K^-) =$

$(8.5 \pm 0.6_{-3.6}^{+2.7}) \times 10^{-4}$ , where the first errors are statistical and the second are systematic. These parameters are not compatible with any known meson resonances.

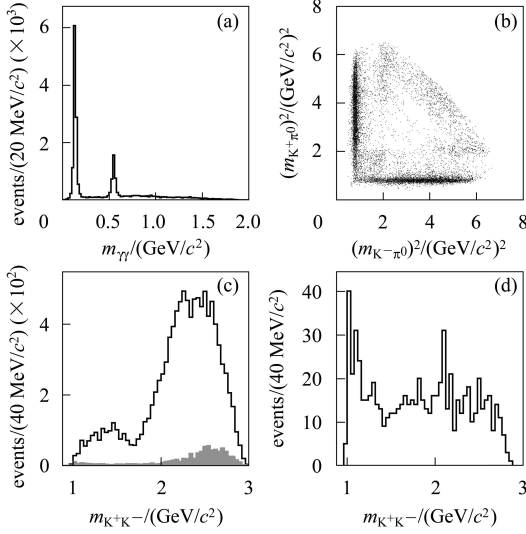


Fig. 4. (a) The  $\gamma\gamma$  invariant mass distribution. (b) The Dalitz plot for  $K^+K^-\pi^0$  candidate events. (c) The  $K^+K^-$  invariant mass distribution for  $K^+K^-\pi^0$  candidate events; the solid histogram is data and the shaded histogram is the background (normalized to data). (d) The  $K^+K^-$  invariant mass distribution for the  $\pi^0$  mass sideband events (not normalized).

To understand the nature of the broad  $1^{--}$  peak, it is important to search for a similar structure in  $J/\psi \rightarrow K_S K^\pm \pi^\mp$  decays to determine its isospin. It is also intriguing to search for  $K^*K, KK\pi$  decay modes. In the mass region of the X, there are several other  $1^{--}$  states, such as the  $\rho(1450)$  and  $\rho(1700)$ , but the width of the X is much broader than the widths of these other mesons. This may be an indication that the X has a different nature than these other mesons. For example, very broad widths are expected for multi-quark states.

#### 4 Partial wave analysis (PWA) of $J/\psi \rightarrow \gamma\pi^+\pi^-$ and $\gamma\pi^0\pi^0$

BES reported the results on  $J/\psi$  radiative decays to  $\pi^+\pi^-$  and  $\pi^0\pi^0$  based on a sample of 58 M  $J/\psi$  events taken with the BES II detector<sup>[9]</sup>. Fig. 5 shows the  $\pi^+\pi^-$  mass spectrum for the selected events, together with the corresponding background distributions and the Dalitz plot. There is a strong  $\rho^0(770)$  peak mainly due to background from  $J/\psi \rightarrow \rho^0\pi^0$ . A strong  $f_2(1270)$  signal, a shoulder on the high mass side of the  $f_2(1270)$ , an enhancement at  $\sim 1.7 \text{ GeV}/c^2$ , and a peak at  $\sim 2.1 \text{ GeV}/c^2$  are clearly visible. The

lightly shaded histogram in Fig. 5 corresponds to the dominant background  $J/\psi \rightarrow \pi^+\pi^-\pi^0$ . The other backgrounds are shown as the dark shaded histogram in Fig. 5. Fig. 6 shows the  $\pi^0\pi^0$  mass spectrum and the Dalitz plot. The shaded histogram corresponds to the sum of estimated backgrounds determined using PDG branching ratios<sup>[10]</sup>. In general, the  $\pi^+\pi^-$  and  $\pi^0\pi^0$  mass spectra exhibit similar structures above  $1.0 \text{ GeV}/c^2$ .

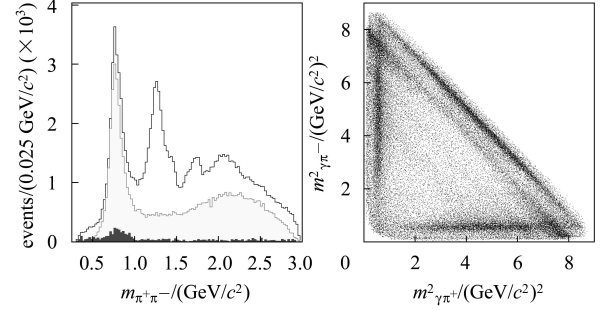


Fig. 5. Invariant mass spectrum of  $\pi^+\pi^-$  and the Dalitz plot for  $J/\psi \rightarrow \gamma\pi^+\pi^-$ , where the lightly and dark shaded histograms in the upper panel correspond to  $J/\psi \rightarrow \pi^+\pi^-\pi^0$  and other estimated backgrounds, respectively.

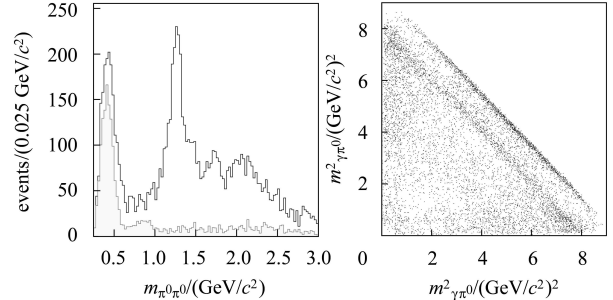


Fig. 6. Invariant mass spectrum of  $\pi^0\pi^0$  and the Dalitz plot for  $J/\psi \rightarrow \gamma\pi^0\pi^0$ , where the shaded histogram in the upper panel corresponds to the estimated backgrounds.

Partial wave analyses (PWA) are carried out using the relativistic covariant tensor amplitude method in the  $1.0$  to  $2.3 \text{ GeV}/c^2$   $\pi\pi$  mass range. There are conspicuous peaks due to the  $f_2(1270)$  and two  $0^{++}$  states in the  $1.45$  and  $1.75 \text{ GeV}/c^2$  mass regions. The first  $0^{++}$  state has a mass of  $1466 \pm 6 \pm 20 \text{ MeV}/c^2$ , a width of  $108_{-11}^{+14} \pm 25 \text{ MeV}/c^2$ , and a branching fraction  $\mathcal{B}(J/\psi \rightarrow \gamma f_0(1500) \rightarrow \gamma\pi^+\pi^-) = (0.67 \pm 0.02 \pm 0.30) \times 10^{-4}$ , which is considered as  $f_0(1500)$ . Spin 0 is strongly preferred over spin 2.

#### 5 Observation of $K^-\bar{\Lambda}$ mass threshold enhancement in $J/\psi \rightarrow pK^-\bar{\Lambda}$

The Dalitz plot for  $J/\psi \rightarrow pK^-\bar{\Lambda}$  events is shown in Fig. 7. In addition to bands for the well established  $\Lambda^*(1520)$ ,  $\Lambda^*(1690)$  and a  $p\bar{\Lambda}$  mass enhancement, isolated from the  $\Lambda^*$  and  $N^*$  bands, in the

right-upper part of the Dalitz plot, there is a significant  $N^*$  band near the  $K^-\bar{\Lambda}$  mass threshold. Fig. 8 shows the invariant mass spectrum of  $K^-\bar{\Lambda}$ . We have performed very preliminary partial wave analysis (PWA) and obtained the mass of this threshold structure  $N_X^*$  in the range of 1500 to 1650  $\text{MeV}/c^2$ , the width about 70 to 110  $\text{MeV}/c^2$  and the spin-parity favoring  $1/2^-$ . In particular, it has a branching ratio  $B(J/\psi \rightarrow \bar{p}N_X^*)B(N_X^* \rightarrow K^-\bar{\Lambda})$  larger than  $2 \times 10^{-4}$ . Considering the mass of  $N_X^*$  is below or very close to  $K^-\bar{\Lambda}$  threshold, i.e., the phase space producing  $K^-\bar{\Lambda}$  final state is very small, the large branching ratio to  $K^-\bar{\Lambda}$  indicates  $N_X^*$  has very strong coupling to  $K^-\bar{\Lambda}$ , suggesting that it could be the  $K^-\bar{\Lambda}$  resonant state predicted by chiral  $SU(3)$  quark model<sup>[11]</sup>.

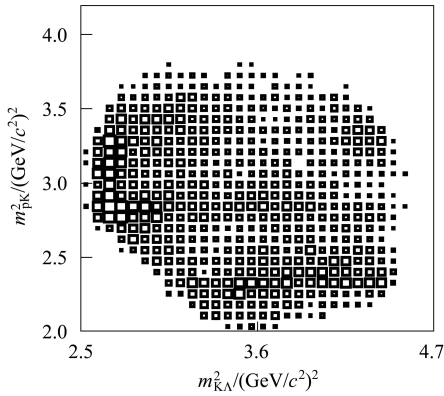


Fig. 7. The Dalitz plot for  $J/\psi \rightarrow pK^-\bar{\Lambda}$ .

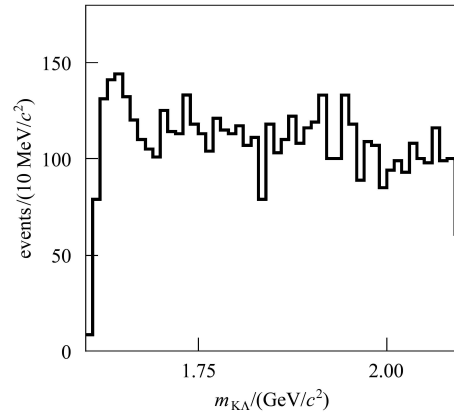


Fig. 8. The  $K^-\bar{\Lambda}$  invariant mass spectrum in  $J/\psi \rightarrow pK^-\bar{\Lambda}$ .

## 6 Summary

With BESII  $5.8 \times 10^7 J/\psi$  data, the  $Y(2175)$  is observed in  $\phi f_0(980)$  mass spectrum in  $J/\psi \rightarrow \eta \phi f_0(980)$ , with the statistical significance of around  $5\sigma$ . The measured mass and width are consistent with those of from BABAR. A broad  $1^{--}$  resonance of  $K^+K^-$  mass in  $J/\psi \rightarrow K^+K^-\pi^0$ , a  $K^-\bar{\Lambda}$  enhancement in  $J/\psi \rightarrow pK^-\bar{\Lambda}$  and the results from the partial wave analysis of  $J/\psi \rightarrow \gamma\pi^+\pi^-$  and  $\gamma\pi^0\pi^0$  are also presented.

## References

- 1 BABAR Collaboration. Phys. Rev. D, 2006, **74**: 091103(R)
- 2 BABAR Collaboration. Phys. Rev. D, 2007, **76**: 031102
- 3 Aubert B et al (BABAR Collaboration). Phys. Rev. Lett., 2005, **95**: 142001
- 4 DING Gui-Jun, YAN Mu-Lin. Phys. Lett. B, 2007, **650**: 390—400
- 5 DING Gui-Jun, YAN Mu-Lin. hep-ph/0701047
- 6 WANG Zhi-Gang. Nucl. Phys. A, 2007, **791**: 106—116
- 7 BES Collaboration. Nucl. Instrum. Methods A, 2001, **458**: 627
- 8 BES Collaboration. Phys. Rev. Lett., 2006, **97**: 142002
- 9 BES Collaboration. Phys. Lett. B, 2006, **642**: 441
- 10 YAO W M et al (Particle Data Group). J. Phys. G: Nucl. Part. Phys., 2006, **33**: 1
- 11 HUANG F, ZHANG Z Y. Phys. Rev. C, 2005, **72**: 024003